Volume 9, Issue 2, 092511 (1-9)

Signal Processing and Renewable Energy (SPRE)

https://doi.org/10.57647/j.spre.2025.0902.11

A density functional theory study of electronic and optical properties of armchair and zigzag silicon carbide nanosheets

Ghobad Mohammad Karimi[1], Mohammad Azim Karami[2],
Hassan Ghalami Bavil Olyaee[3,*], Javad Karamdel[1]

[1] *Department of Electrical Engineering, south Tehran Branch, Islamic Azad University, Tehran, Iran.*
[2] *School of Electrical Engineering, Iran University of Science & Technology (IUST), Tehran, Iran.*
[3] *Department of Physics, South Tehran Branch, Islamic Azad University, Tehran, Iran.*

*__Corresponding author:__ olyaee@iau.ac.ir

Original Research

Received:
12 February 2025
Revised:
9 March 2025
Accepted:
17 March 2025
Published online:
1 June 2025

© 2025 The Author(s). Published by the OICC Press under the terms of the Creative Commons Attribution License, which permits use, distribution and reproduction in any medium, provided the original work is properly cited.

Abstract:

Using the density functional theory (DFT) based on first principles calculations, the two-dimensional (2D) nanostructure of silicon carbide (SiC) is investigated in this article. The band structure, density of states, and optical properties of 2D armchair (n,n) and zigzag $(n,0)$ nanostructures ($n = 3, 4, 5$) are calculated. Calculations show that the introduced nanostructures have a direct energy gap of 2.82 electron volts (eV), a valence band edge of nearly -1.38 eV, and a conduction band edge of almost 1.44 eV. Also, the calculations show that in armchair silicon carbide nanosheets (ASiCNSs) (3, 3) at the point of 3.55 electron volts, the absorption coefficient is 432466 cm^{-1}, which is the highest absorption coefficient among all studied structures in this paper.

Keywords: SiC; DFT; Electronic and optical properties; Armchair and zigzag

1. Introduction

Finding and engineering new materials with new electronic and optical properties is crucial in the development of new electro-optical devices. After the discovery of graphene in the last half century [1], the unique properties of this 2D structure of carbon caused extensive studies to be conducted to find novel 2D nanostructures [2]. In [3], SiC nanostructures, including clusters/nanocrystals, nanowires, nanotubes, and nanosheets have been investigated by the DFT method. Important results of silicon carbide nanosheets fully describe their structure, electronic, optical, magnetic, mechanical properties, and device applications [4].

In [5], the electronic properties of single-layer silicon carbide plates doped with transition metals have been investigated using DFT. In [6], the electronic, optical, and electrical conductivity properties of two single-layer tetragonal silicon carbides have been studied using DFT and Boltzmann's theory. In [7], silicon carbide nanosheet optical and electronic properties with hydrogen absorption have been studied by the DFT method. It is found that the valence band edge of the structure is mostly influenced by the orbitals of carbon atoms while the conduction band edge is partially influenced by the orbitals of silicon atoms. In [8], both mean field methods (Cohensham DFT energies) and advanced methods with Green's function have been used to study the electronic band structure and optical properties of SiC nanostructures. In [9], the magnetic, electronic, and optical properties of nine silicon carbide systems doped by non-metals have been systematically investigated by DFT. In [10], The effect of fluorination on the electronic, optical, magnetic and stability properties of silicon carbide nanosheets has been investigated using the DFT method. The absorption of F atoms leads to changes in the optical properties of the spectrum. In [11], the mechanical properties of thirteen types of Si_mC_n nanosheets have been investigated using density functional theory. In [12], a two-dimensional nanostructure of silicon carbide, which has stable mechanical and thermodynamic properties, is proposed. In [13], a comprehensive structural search has been performed on the 2D sheet Si_xC_{1-x} with $0 < x < 1$ using the cluster expansion method in connection with DFT calculations. In [14], the effects of Spin–Orbit Coupling (SOC) on the 2D electronic structure of SiC have been systematically investigated by DFT theory. The results show that the 2D structure of SiC is a graphene-like hexagonal network with superior structural and dynamic stability. In [15], a three-dimensional finite element model based on molecular mechanics was used to study the stability behavior of single-layer SiC nanosheets (SLSiCNS). The bonds between silicon and carbon atoms are simulated by structural beam elements. In [16], the heat effect on the mechanical properties of SiC graphene sheet has been studied using DFT and phonon energy, using quasi-harmonic approximation (QHA) code based on DFT calculation with generalized gradient approximation (GGA).

In section 2, the material and method are explained. In section 3, electronic properties, and in section 4, optical spectrum is described. In the end, a summary of the results is explained in section 5.

2. Material and method

The electronic and optical properties of SiC sheets using the DFT method at room temperature are simulated in this research. In this paper, The exchange-correlation potential is HSE06 in hybrid generalized-gradient approximation (hybrid GGA) [17–22] as the exchange-correlation functional are performed using the DFT package. The pseudopotential, FHI, is considered. Double zeta polarization (DZP) basis sets and is used with a mesh cutoff, about 75 Hartree. The *k*-points in Brillouin zone integration, number of atoms, and Tetragonal unit cell, with equilibrium lattice constants, depend on the structure (which is mentioned in Table 1).

Table 1. The number of atoms, lattice parameters, and sampling of structure.

Structure	Number of atoms	Lattice parameters	Sampling
(3,0)	60	X=10.00 Y=09.67 Z=27.90	(1,6,20)
(4,0)	80	X=10.00 Y=12.89 Z=27.90	(1,8,20)
(5,0)	100	X=10.00 Y=16.11 Z=27.90	(1,10,20)
(3,3)	60	X=10.00 Y=16.74 Z=16.11	(1,12,10)
(4,4)	80	X=10.00 Y=22.32 Z=16.11	(1,16,10)
(5,5)	100	X=10.00 Y=27.90 Z=16.11	(1,20,10)

Initially, to optimize the sheets, the force tolerance is 0.001 eV/Å, and the optimizer method is LBFGS. Then, the electronic and optical properties of sheets are calculated, and a bond distance of 1.86 Å [23] is chosen as the proper model (Fig. 1). The silicon and carbon atoms are represented by yellow and grey balls, respectively.

To check the accuracy of the results, [23] is considered as the main structure, in which the band gap for the perfect state is 2.01 eV. This close agreement (difference of 0.08 eV) between our result and [23] suggests that the simulation setup is valid.

3. Electronic properties

Fig. 2 shows the band structures of the studied six structures. The Fermi level is set to the energy zero. Therefore, the positive energy levels are the conduction band and the negative energy levels are the valence band. The band gap value is the same in all six structures due to the absence of defects and doping. The band structures show that the energy band gap is 2.82 eV which means that all structures are semiconductors. This band gap can encourage us to simulate photodetectors based on two-dimensional silicon carbide materials. Furthermore, the band structures suggest that the zigzag and armchair SiCNSs are direct-gap semiconductors. Band gap, Valence band edge, and Conduction

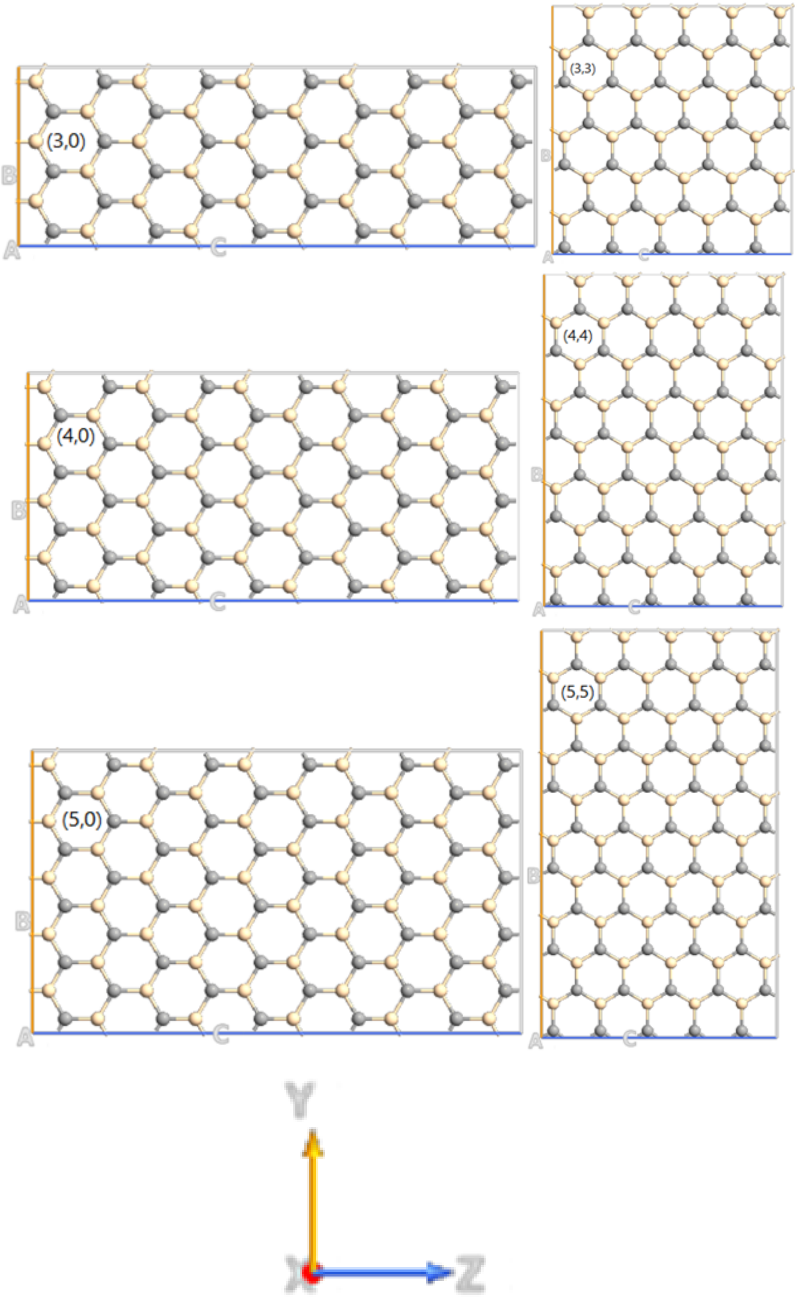

Figure 1. Schematic view of six different simulated SiCNS- structures at XYZ plane. Yellow and gray spheres are used to represent silicon and carbon atoms, respectively.

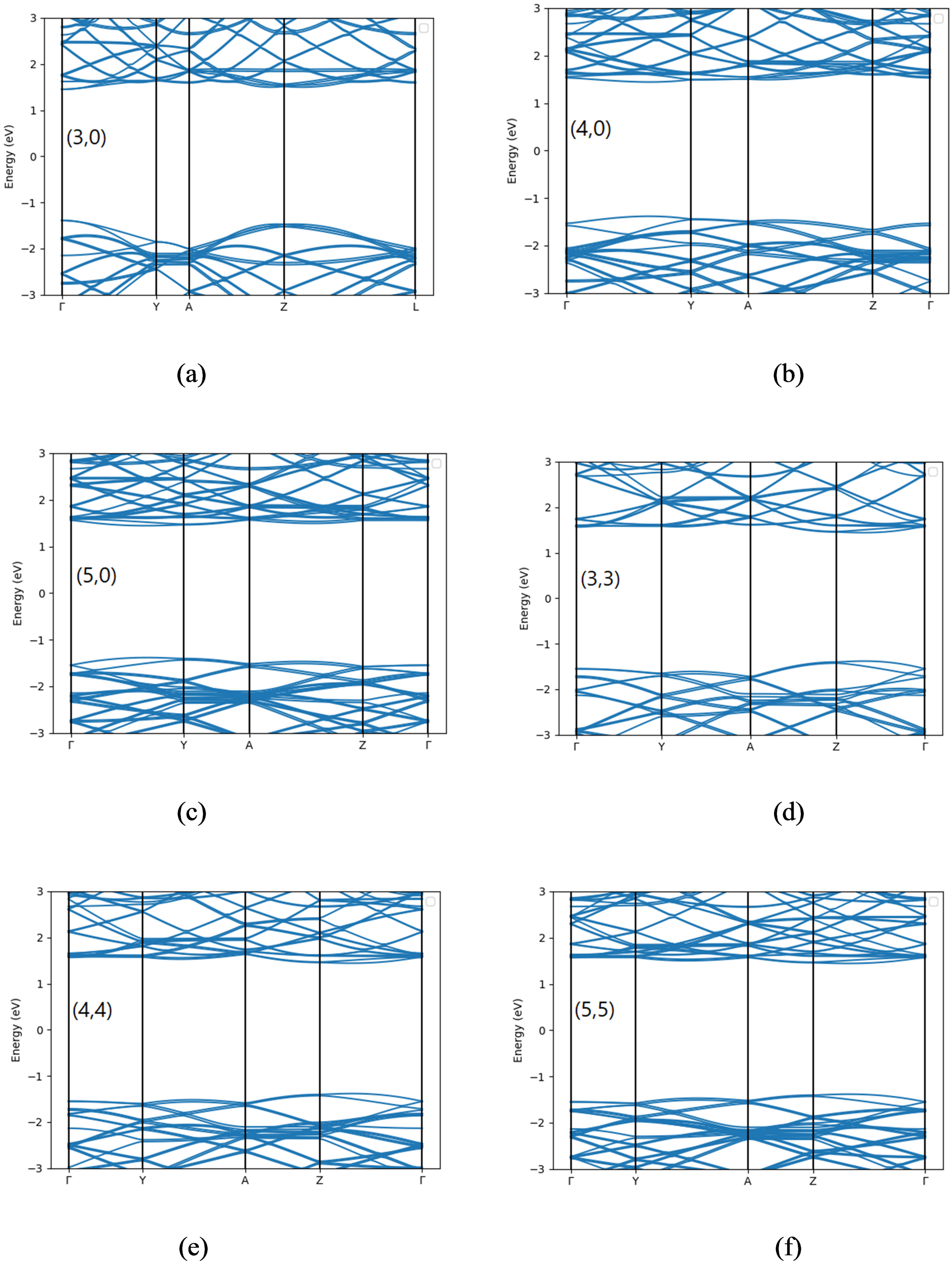

(a) (b)

(c) (d)

(e) (f)

Figure 2. Band structure of (a) ZSiCNSs (3,0), (b) ZSiCNSs (4,0), (c) ZSiCNSs (5,0), (d) ASiCNSs (3,3), (e) SiCNSs (4,4), and (f) ASiCNSs (5,5).

band edge values are indicated in Table 2.

The distribution of electrons in the energy spectrum is described by the density of states and can be measured in light absorption experiments. To determine the electronic properties of solids, it is essential to examine the general density of states around the Fermi level. By comparing the general densities of compounds with the general densities of each of the atoms in the compound, the states that are effective in-electric conduction can be determined [24]. Fig. 3 shows the density of state of the six structures studied, which represents the number of the states per unit of energy. It has been observed that the density of states is higher in larger structures.

Table 2. Direct or indirect type, band gap result, valence band edge, conduction band edge of studied structures.

Structure	Direct or indirect	Band gap (eV)	Valence band edge(eV)	Conduction band edge(eV)
(3,0)	Direct	2.84162	-1.39021	1.45142
(4,0)	Direct	2.82776	-1.38500	1.44276
(5,0)	Direct	2.82994	-1.38562	1.44432
(3,3)	Direct	2.82371	-1.38282	1.44090
(4,4)	Direct	2.82696	-1.38436	1.44260
(5,5)	Direct	2.82830	-1.38499	1.44331

4. Optical spectrum

To analyze the optical spectrum, we calculate the optical absorption coefficient by first determining the electric susceptibility. The electric susceptibility is a dimensionless proportionality constant describing how a material responds to an external electric field [25]. In this study, we utilize the Kubo-Greenwood equation to compute the susceptibility tensor, which serves as the basis for determining the optical properties of the material [25, 26]. The Kubo-Greenwood equation is given by

$$\chi_{ij}(\omega) = \frac{e^2}{m_e^2 V}\sum_{nmk}\frac{f_{nk}-f_{mk}}{\hbar\omega_{nm}-\hbar\omega-i\Gamma}|<n,k|p_i|m,k>|^2 \tag{1}$$

where:

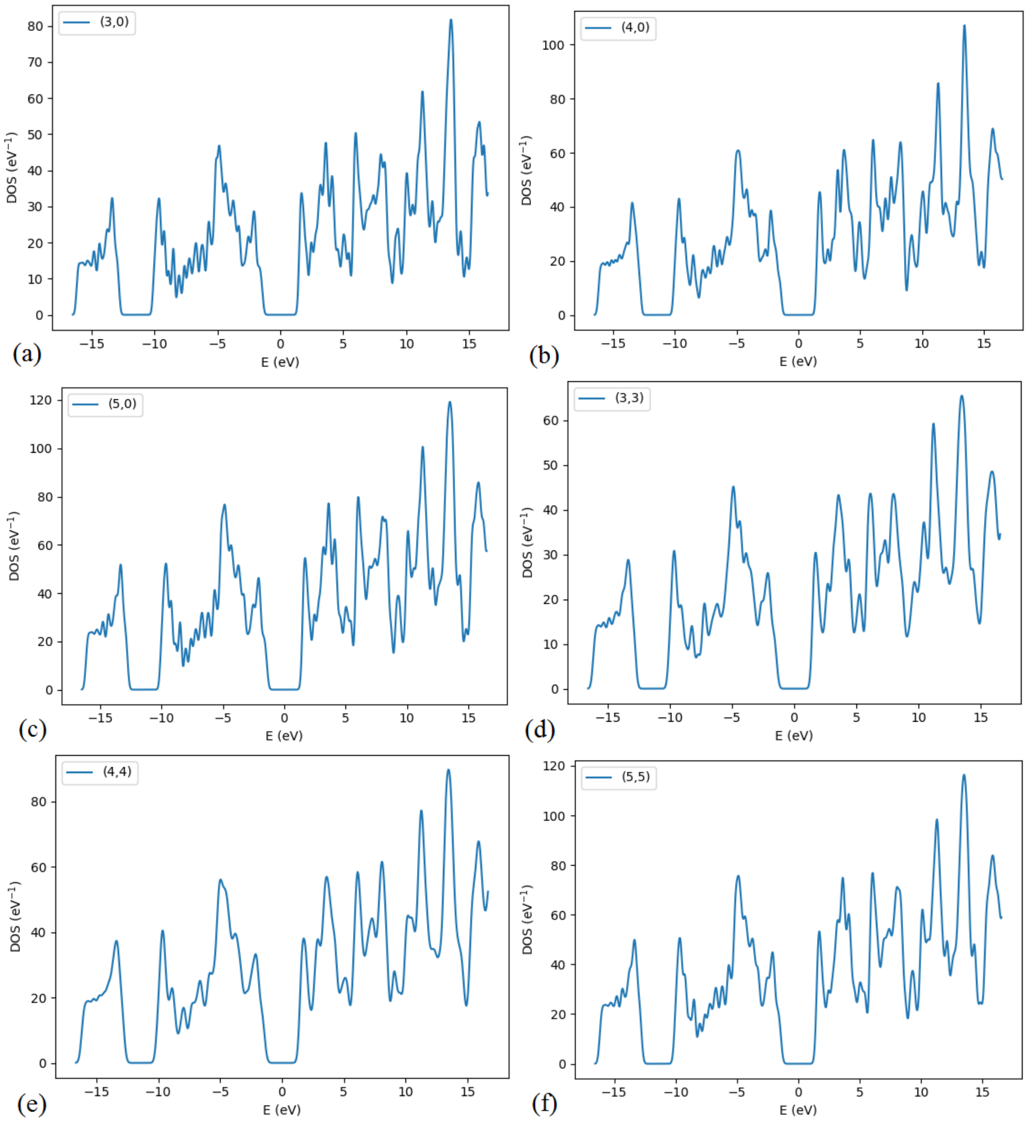

Figure 3. Density of state of (a) ZSiCNSs (3,0), (b) ZSiCNSs (4,0), (c) ZSiCNSs (5,0), (d) ASiCNSs (3,3), (e) SiCNSs (4,4), and (f) ASiCNSs (5,5).

- $\chi_{ij}(\omega)$: The susceptibility tensor component at frequency ω.
- e: Electron charge.
- p_i: The momentum operator component between states n and m.
- m_e: Electron mass.
- V: Volume of the material.
- Γ: Energy broadening, a parameter accounting for the finite lifetimes of excited states.
- $\hbar\omega_{nm}$: Energy difference between states n and m ($\hbar$ is the reduced Planck constant).
- f_{nk}: Fermi function evaluated at the band energy $E_n(k)$.
- k: Crystal momentum

To ensure an accurate evaluation of the optical absorption coefficient, the following considerations are made:
The relative dielectric constant, ε_r is related to the susceptibility by [27], [28]:

$$\varepsilon_r(\omega) = (1+\chi(\omega)) \tag{2}$$

The derivation of relation (2) can be found in [29]. The static (low frequency) dielectric response $\varepsilon(\omega) = \varepsilon_0\varepsilon_r(\omega)$ which consists of two parts: electronic and ionic [30]:

$$\varepsilon_{r,\alpha,\beta} = \varepsilon^{elec}_{r,\alpha,\beta}(\omega) + \varepsilon^{ionic}_{r,\alpha,\beta}(\omega) \tag{3}$$

where ε_r is the unitless relative permittivity and α, β (this paper α and β are YY and ZZ direction) are Cartesian directions. The value of the electronic dielectric constant is obtained by accurate evaluation at zero frequency. So $\varepsilon^{elec}_{r,YY,ZZ}(0)$ is given in Table 3.
which is n refractive index and it is obtained from the following relation [27]:

$$n + i\kappa = \sqrt{\varepsilon_r} \tag{4}$$

here κ is the extinction coefficient. The dielectric constant consists of two parts, real (ε_1) and imaginary (ε_2) [27].

$$n = \sqrt{\frac{\sqrt{\varepsilon_1^2+\varepsilon_2^2}+\varepsilon_1}{2}} \tag{5}$$

$$\kappa = \sqrt{\frac{\sqrt{\varepsilon_1^2+\varepsilon_2^2}-\varepsilon_1}{2}} \tag{6}$$

The optical absorption coefficient is obtained from the extinction coefficient relationship [31]

$$\alpha_a = 2\frac{\omega}{c}\kappa \tag{7}$$

where c is the speed of light and ω is the frequency.
As explained in section 3, the six structures introduced are the absence of defects and doping, so as shown in Fig. 4, it is clear that the optical absorption coefficient occurs in a certain range, and the only distinguishing feature in the structures is the maximum value of the optical absorption coefficient, which varies according to the type of structure. Interestingly, the calculations revealed an intriguing light absorption characteristic. The material exhibits zero absorption in the XX direction, while non-zero absorption occurs in the YY and ZZ directions. In the yy and ZZ directions, absorption starts at 2 eV and extends up to 5 eV, reaching its peak intensity between $3-4$ eV.

Table 3. The ε_r for the studied structures.

Structure	$\varepsilon_{r,YY}(0)$	$\varepsilon_{r,ZZ}(0)$
(3,0)	1.34	1.39
(4,0)	1.24	1.34
(5,0)	1.25	1.26
(3,3)	1.40	1.47
(4,4)	1.30	1.38
(5,5)	1.25	1.27

5. Conclusions

Using density functional theory, this paper studied the electronic and optical properties of silicon carbide sheets. Various armchair and zigzag SiCNSs structures are investigated. The band gap, density of state, dielectric constant, and optical absorption are computed. From the band structure, it is found that the band gap energy is almost 2.82 eV. Hence compounds can be used in nanoelectronics and optoelectronics industry due to their wide band gap. The DOS figure shows that the density of states is higher in armchair and zigzag SiCNSs (5,0) and (5,5). The optical absorption spectrum reveals significant absorption in the energy range of $2-5$ eV, corresponding to the ultraviolet-visible (UV-Vis) region, which enhances its suitability for applications in optoelectronic devices.

Authors contributions
Authors have contributed equally in preparing and writing the manuscript.

Availability of data and materials
The data that support the findings of this study are available from the corresponding author upon reasonable request.

Conflict of interests
The authors declare that they have no known competing financial interests or personal relationships that could have appeared to influence the work reported in this paper.

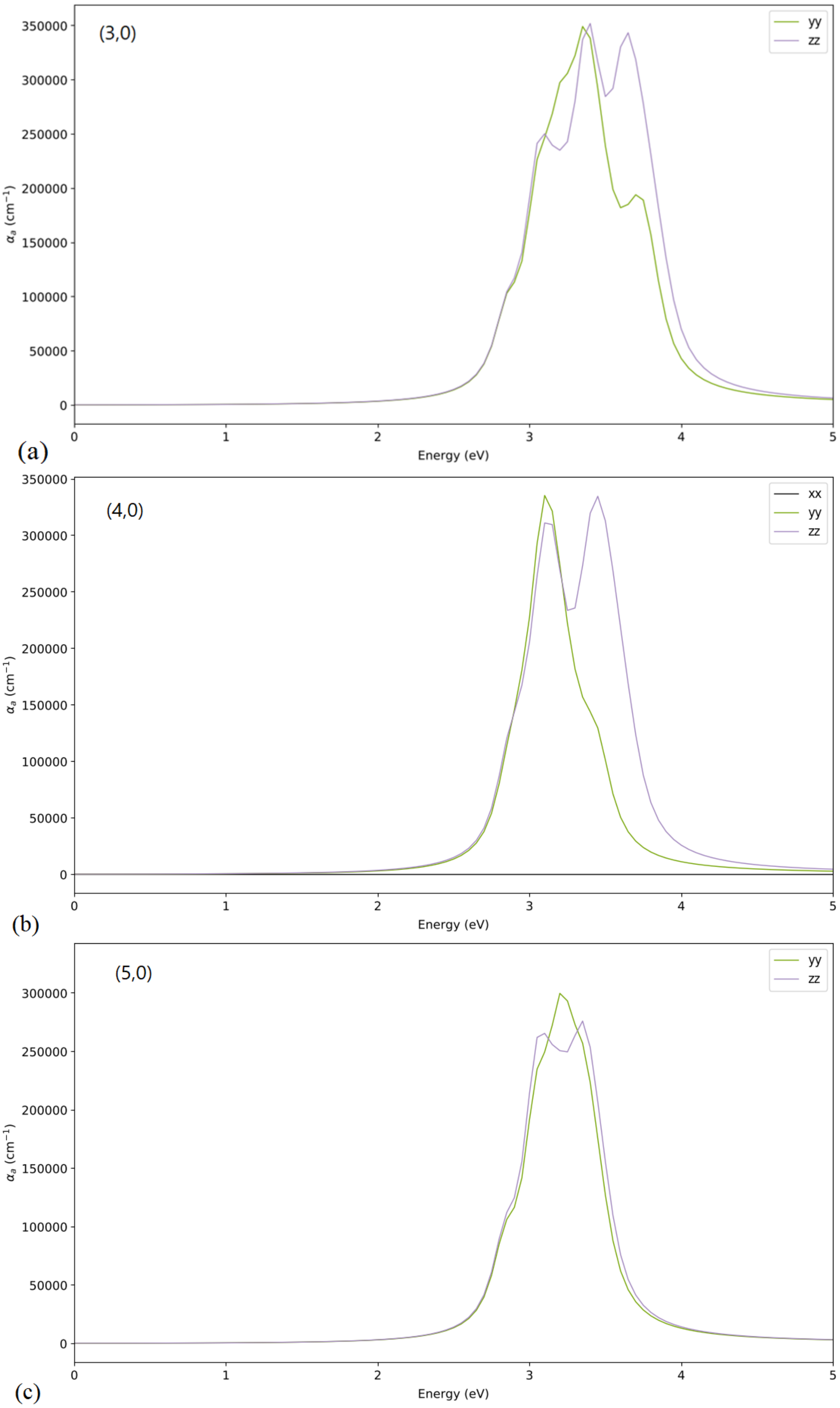
(3,0)
yy
zz
α_a (cm^{-1})
350000
300000
250000
200000
150000
100000
50000
0
0
1
2
3
4
5
Energy (eV)
(a)
(4,0)
xx
yy
zz
α_a (cm^{-1})
350000
300000
250000
200000
150000
100000
50000
0
0
1
2
3
4
5
Energy (eV)
(b)
(5,0)
yy
zz
α_a (cm^{-1})
300000
250000
200000
150000
100000
50000
0
0
1
2
3
4
5
Energy (eV)
(c)

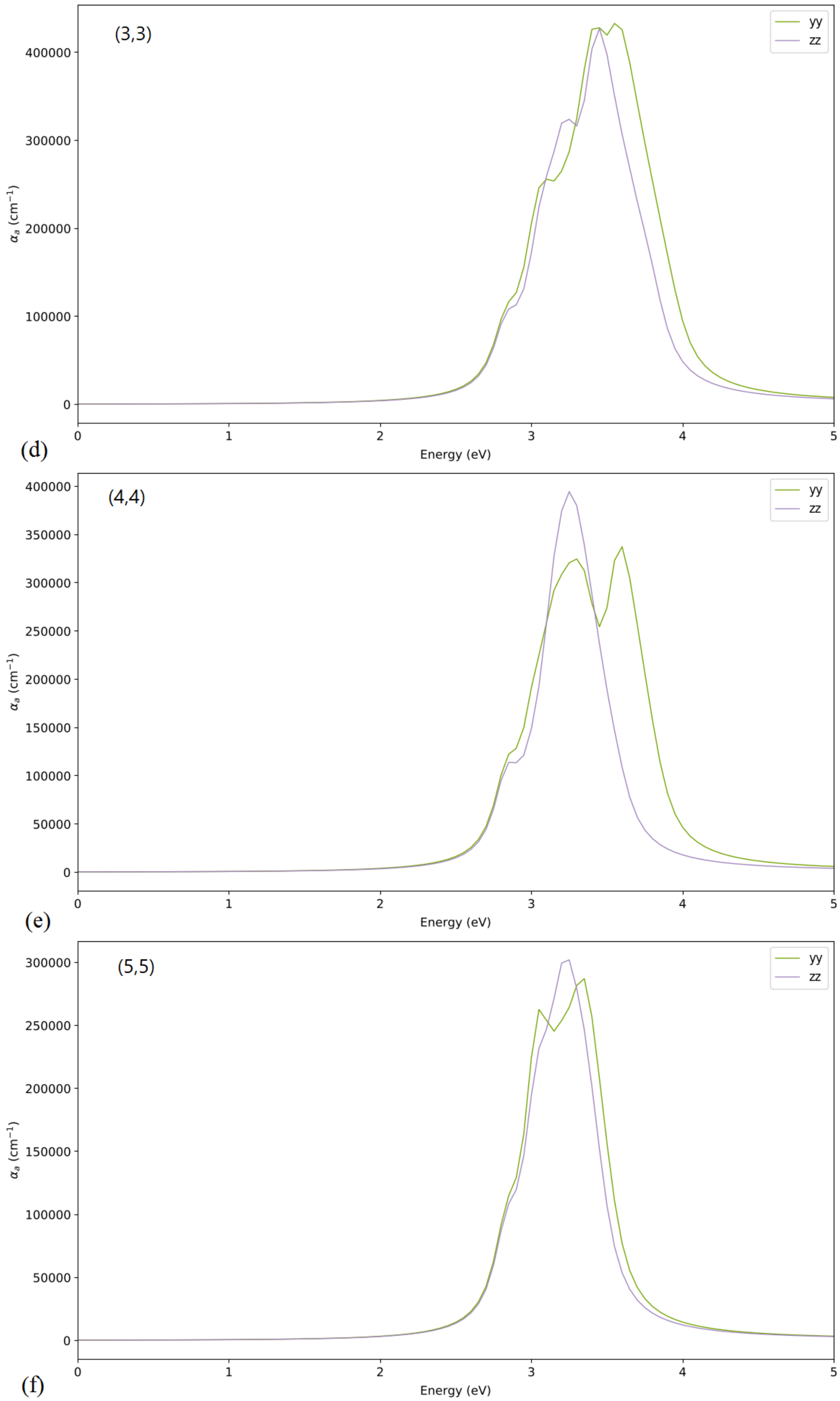

Figure 4. Optical absorption of (a) ZSiCNSs (3,0), (b) ZSiCNSs (4,0), (c) ZSiCNSs (5,0), (d) ASiCNSs (3,3), (e) SiCNSs (4,4), and (f) ASiCNSs (5,5).

References

[1] K. S. Novoselov et al. “Electric field effect in atomically thin carbon films.”. *Science*, 306(5696):666–669, 2004.
DOI: https://doi.org/10.1126/science.1102896.

[2] “Semiconductor-Insulator–Semiconductor Diode Consisting of Monolayer MoS2, h-BN, and GaN Heterostructure.”. *ACS Nano*, 2023.
DOI: https://doi.org/10.1021/acsnano.5b04233.

[3] Y. Zhao, T. Hou, L. Wu, Y. Li, and S.-T. Lee. “Density Functional Calculations on Silicon Carbide Nanostructures.”. *J. Comput. Theor. Nanosci*, 9(11):1980–1998, 2012.
DOI: https://doi.org/10.1166/jctn.2012.2604.

[4] S. Chabi and K. Kadel. “Two-Dimensional Silicon Carbide: Emerging Direct Band Gap Semiconductor.”. *Nanomaterials*, 10(11), 2020.
DOI: https://doi.org/10.3390/nano10112226.

[5] “A density functional theory study of electronic properties of transition metals doped silicon carbide monolayer.”. *International Journal of Quantum Chemistry - Wiley Online Library*, 2022.
DOI: https://doi.org/10.1002/qua.26877.

[6] M. Houmad, O. Dakir, M. H. Mohammed, M. Khuili, A. El Kenz, and A. Benyoussef. “Electronic and electrical properties of two single-layer tetragonal silicon carbides.”. *Chem. Phys. Lett.*, 754: 137710, 2020.
DOI: https://doi.org/10.1016/j.cplett.2020.137710.

[7] N. Delavari and M. Jafari. “Electronic and optical properties of hydrogenated silicon carbide nanosheets: A DFT study.”. *Solid State Commun.*, 275:1–7, 2018.
DOI: https://doi.org/10.1016/j.ssc.2018.03.004.

[8] H.-C. Hsueh, G.-Y. Guo, and S. G. Louie. “Electronic and Optical Properties of Silicon Carbide Nanostructures.”. *Silicon-based Nanomaterials*, pages 139–159, 2013.
DOI: https://doi.org/10.1007/978-1-4614-8169-0-7.

[9] “Frontiers — Electronic, Magnetic, and Optical Performances of Non-Metals Doped Silicon Carbide.”. 2023.
DOI: https://doi.org/10.3389/fchem.2022.898174/full.

[10] J. A. Gonçalves, O. F. P. dos Santos, R. J. C. Batista, and S. Azevedo. “First-principle investigation of silicon carbide nanosheets fluorination: Stability trends, electronic, optical and magnetic properties.”. *Chem. Phys. Lett.*, 787:139266, 2022.
DOI: https://doi.org/10.1016/j.cplett.2021.139266.

[11] “Mechanical properties of various two-dimensional silicon carbide sheets: An atomistic study.”. *Superlattices Microstruct*, 98:102–115, 2016.
DOI: https://doi.org/10.1016/j.spmi.2016.08.003.

[12] Q. Wei, Y. Yang, G. Yang, and X. Peng. “New stable two dimensional silicon carbide nanosheets.”. *J. Alloys Compd.*, 868:159201, 2021.
DOI: https://doi.org/10.1016/j.jallcom.2021.159201.

[13] Z. Shi, Z. Zhang, A. Kutana, and B. I. Yakobson. “Predicting Two-Dimensional Silicon Carbide Monolayers.”. *ACS Nano*, 9(10):9802–9809, 2015.
DOI: https://doi.org/10.1021/acsnano.5b02753.

[14] Md. R. Islam, Md. S. Islam, N. Ferdous, K. N. Anindya, and A. Hashimoto. “Spin-orbit coupling effects on the electronic structure of two-dimensional silicon carbide.”. *J. Comput. Electron.*, 18 (2):407–414, 2019.
DOI: https://doi.org/10.1007/s10825-019-01326-2.

[15] R. Ansari, S. Rouhi, M. Mirnezhad, and M. Aryayi. “Stability characteristics of single-layered silicon carbide nanosheets under uniaxial compression.”. *Phys. E Low-Dimens. Syst. Nanostructures*, 53:22–28, 2013.
DOI: https://doi.org/10.1016/j.physe.2013.04.014.

[16] M. Faghihnasiri, M. Rezvani, M. Shabani, and A. H. Firouzian. “The temperature effect on mechanical properties of silicon carbide sheet based on density functional treatment.”. *Solid State Commun.*, 227: 40–44, 2016.
DOI: https://doi.org/10.1016/j.ssc.2015.11.014.

[17] J. Hermet, C. Adamo, and P. Cortona. “Towards a Greater Accuracy in DFT Calculations: From GGA to Hybrid Functionals.”. *Quantum Simulations of Materials and Biological Systems*, pages 3–15, 2012.
DOI: https://doi.org/10.1007/978-94-007-4948-1-1.

[18] R. Peverati and D. G. Truhlar. “Improving the Accuracy of Hybrid Meta-GGA Density Functionals by Range Separation.”. *J. Phys. Chem. Lett.*, 2(21):2810–2817, 2011.
DOI: https://doi.org/10.1021/jz201170d.

[19] L. Simón and J. M. Goodman. “How reliable are DFT transition structures? Comparison of GGA, hybrid-meta-GGA and meta-GGA functionals.”. *Org. Biomol. Chem.*, 9(3):689–700, 2011.
DOI: https://doi.org/10.1039/C0OB00477D.

[20] Y. Zhao and D. G. Truhlar. “The M06 suite of density functionals for main group thermochemistry, thermochemical kinetics, noncovalent interactions, excited states, and transition elements: two new functionals and systematic testing of four M06-class functionals and 12 other functionals.”. *Theor. Chem. Acc.*, 120(1):215–241, 2008.
DOI: https://doi.org/10.1007/s00214-007-0310-x.

[21] M. G. Medvedev, I. S. Bushmarinov, J. Sun, J. P. Perdew, and K. A. Lyssenko. “Density functional theory is straying from the path toward the exact functional.”. *Science*, 2017.
DOI: https://doi.org/10.1126/science.aah5975.

[22] Y. Zhao and D. G. Truhlar. “Density Functional for Spectroscopy: No Long-Range Self-Interaction Error, Good Performance for Rydberg and Charge-Transfer States, and Better Performance on Average than B3LYP for Ground States.”. *J. Phys. Chem. A*, 110(49):13126–13130, 2006.
DOI: https://doi.org/10.1021/jp066479k.

[23] E. Zaminpayma. “A density functional theory study of electric, magnetic and optical properties of perfect and defected Germanium Carbide (GeC) sheet.”. *Comput. Condens. Matter*, 26:e00533, 2021.
DOI: https://doi.org/10.1016/j.cocom.2020.e00533.

[24] B. Streetman and S. Banerjee. “Solid State Electronic Devices.”. *Boston: Pearson*, 2014.

[25] J. E. Sipe and E. Ghahramani. “Nonlinear optical response of semiconductors in the independent-particle approximation.”. *Phys. Rev. B*, 48(16):11705–11722, 1993.
DOI: https://doi.org/10.1103/PhysRevB.48.11705.

[26] W. A. Harrison. “Solid State Theory.”. 1970.

[27] W. A. Harrison. “Solid state theory.”. 1970. URL http://archive.org/details/solidstatetheory0000harr.

[28] H. Alborznia and S. T. Mohammadi. “Biaxial stress and strain effects on optical and electronic aspects of B2C nanostructure: a first-principles calculation.”. *Indian J. Phys.*, 96(11):3117–3123, 2022.
DOI: https://doi.org/10.1007/s12648-021-02272-1.

[29] D. J. Griffiths. “Introduction to Electrodynamics.”. *Upper Saddle River, N.J: Prentice Hall*, 1999.

[30] X. Gonze and C. Lee. “Dynamical matrices, Born effective charges, dielectric permittivity tensors, and interatomic force constants from density-functional perturbation theory.”. *Phys. Rev. B*, 55(16):10355–10368, 1997.
DOI: https://doi.org/10.1103/PhysRevB.55.10355.

[31] A. Glisson and R. W. Scharstein. “Introduction to electrodynamics.”. *IEEE Antennas Propag. Mag.*, 43(1), 2001.
DOI: https://doi.org/10.1109/MAP.2001.920021.